Sustainable Structures
ISSN: 2789-3111 (Print); ISSN: 2789-312X (Online)
http://www.sustain-dpl.com/picnews.asp?id=155
DOI: 10.54113/j.sust.2023.000021

ORIGINAL ARTICLE

Structural responses of FRP sheet piles under cantilever loading

Joshua Wilt[a], Ruifeng Liang[a], Hota GangaRao[a,*], Jeremy Mostoller[b]

[a] NSF I/UCRC for Integration of Composites into Infrastructure and Constructed Facilities Center, West Virginia University, Morgantown, WV, USA
[b] Creative Composites Group, Creative Pultrusions, 214 Industrial Lane, Alum Bank, PA, USA
[*]Corresponding Author: Hota Gangarao, Email: hota.gangarao@mail.wvu.edu.

Abstract: Sheet piles are interlocked segments used for temporary or permanent soil and water retaining structures such as below-grade parking structures and sea walls. Although steel is commonly used due to its strength and ease of manufacturing, it rusts in saltwater. Fiber reinforced polymer (FRP) composite sheet piles are resistant to chlorides and have higher corrosion resistance, but their mechanical properties vary in length and width. Stress risers at corrugation corners make soil-structure interaction a challenging design issue. This research aims to develop a standardized test procedure to determine the resisting moment capacity of FRP composite sheet piles. Cantilevered FRP sheet piles fixed with a sand-concrete mixture of ~70 psi (0.48 MPa) compressive strength were tested under static loads. Strain gages and LVDTs were used to collect data on deformation response up to and beyond peak induced stress. Results suggest that the refined test procedure can assist engineers in designing efficient sheet pile structures and become a basis to develop ASTM standard.

Keywords: Fiber reinforced polymer; composites; piling; sheet pile; testing; structural response; cantilever loading

1 Introduction

Fiber-reinforced polymer (FRP) composites have emerged as promising materials for various applications in infrastructure applications due to their high strength-to-weight ratio, corrosion resistance, and ease of installation, among other advantages. FRP composites are versatile materials manufactured by embedding continuous fibers, such as glass, aramid or carbon, in a polymer matrix. The resulting composite material combines the best attributes of its constituents - the strength and stiffness of the fibers and the ductility of the polymer matrix [1-2]. One of the manufacturing processes known as pultrusion, allows for a continuous production of FRP products, featuring consistent cross sections and high-volume output [3].

Sheet pile walls are commonly used in civil engineering for temporary or permanent structures to retain soil or water and avoid coastal erosion. They are employed in various applications, including riverbank protection, excavation support, seawall construction, and flood control structures [4-7]. Traditional sheet piles are made from materials such as steel or timber, but these materials have their limitations. Steel, for instance, is susceptible to corrosion, especially in aggressive environments like seawater, and results in lower service life. Timber, on the other hand, is prone to decay and has a lower strength-to-weight ratio [1, 8-9].

The use of FRP composites for sheet pile walls, however, offers several advantages. First, they are

Received: 1 December 2022; Received in revised form: 1 January 2023; Accepted: 2 January 2023

resistant to corrosion, which makes them ideal for use in aggressive environments, such as marine or chemical settings [8,10]. Second, they have a high strength-to-weight ratio, which can result in more manageable and efficient installation processes compared to traditional materials [3,10-11]. Third, they offer low life-cycle cost, and approximately 75-year service life. Fourth, their inherent flexibility allows them to better adapt to ground movements, reducing the likelihood of failure under load [12-13]. Lampo et al. [9] emphasized the importance of developing and demonstrating FRP composite systems for various applications, such as fender load-bearing and sheet piling systems. These demonstrations provide tangible proof of the material's effectiveness and reliability, encouraging further adoption of FRP composites in civil engineering. A typical retaining wall made of FRP composite sheet piling is shown in **Fig. 1**.

Fig. 1. Sheet piling of Long Beach, New York (Photo courtesy of Creative Composites group).

The flexural behavior of FRP composite sheet piles is an important consideration in their design and application. Several studies have analyzed the flexural performance of these composites, contributing to a more robust understanding of their behavior under load [3, 12-13]. For example, Wang et al. [3] conducted an analytical and experimental study on the flexural behavior of pultruded FRP sheet piles, while Giroux and Shao [12] focused on the flexural and shear rigidity of composite sheet piles. A similar study was conducted by Shao and Shanmugam [13] on moment capacities and deflection limits of pultruded FRP sheet piles. Their findings proved beneficial in defining the structural behavior of these materials and providing a baseline for further research and applications. In addition, local buckling behavior is a concern when these materials are subjected to uniform pressure [14]. It is worth noting that the failure modes under three-point bending differ from those observed under cantilever loading. The research by Noh et al. [15] and Boscato et al. [16] delves into the dynamic loading conditions, such as impact or seismic activity, and FRP material response.

Durability especially under harsh environments is another crucial factor when considering the use of FRP composite materials in civil engineering [8, 10, 17-19]. Fiberglass composite sheet piles, for instance, have been researched extensively for their durability, especially when in contact with water, to determine their long-term performance. Such studies like those by Fang et al. [10] and Kouadio [19] and are vital, considering many applications of sheet piles are in wet or moist conditions where corrosion or rot can be a significant problem for traditional materials.

The geotechnical properties of the surrounding soil can significantly influence the performance and stability of the sheet pile walls [5-6, 20-24]. For example, El-Hanafy and AbdelAziz [25] studied the effect of using cemented sand as a replacement layer beneath a strip footing, which could have implications for the stability of sheet pile walls. GuhaRay and Baidya [26] explored the reliability-based analysis of cantilever sheet pile walls backfilled with different soil types using the finite-element approach. The study by Das and Sivakugan [5] emphasized the principles of foundation engineering and the vital role that soil mechanics plays in understanding the performance of sheet piles. The work of Madabhushi and Chandrasekaran [27] studied the rotation of cantilever sheet pile walls, a factor that can greatly influence the stability of the structure and that can be affected by soil conditions. Research by authors such as Murthy [20], Das [21] and Terzaghi [28] have provided a solid foundation in this area, but the specifics of how these factors interact with FRP materials are still an active area of research.

The installation method of FRP composite sheet piles is another important aspect that directly affects their performance. Guades et al. [8] conducted a comprehensive review on the driving performance of FRP composite piles, highlighting the need for suitable installation techniques that can accommodate the unique properties of these materials. The authors emphasized that inadequate installation methods could compromise the integrity of the sheet pile wall and ultimately its performance. In addition, the design and installation of FRP sheet piles must also account for various loading conditions, including uniform loads, impact loads, and seismic loads [13, 15-16, 29-30]. The ability of FRP composite sheet piles to withstand these loads is crucial for the safety and stability of the structure. Finite element analysis is often used to understand the behavior of these structures under different loading conditions, as illustrated by the research of Fabien [29], who studied the behavior of composite sheet piles subjected to uniform load and harsh environments. Bilgin [31] conducted numerical studies on anchored sheet pile wall behavior constructed in cut and fill conditions, which provided significant insight into how these structures respond to different stresses. The study by GuhaRay and Baidya [26] is particularly useful for simulating complex scenarios and analyzing the response of FRP sheet piles to various loading conditions. This allows engineers to predict the behavior of sheet piles more accurately and to design them more effectively.

Moreover, the connections of FRP composites in civil infrastructure pose another significant research avenue [32-33]. Fang et al. [10] demonstrated the importance of understanding these connections, especially in aggressive environments. For instance, the corrosive effects of saltwater in coastal regions can seriously compromise the integrity of traditional materials. FRP materials show increased resistance to these corrosive elements, but understanding the long-term effects and potential degradation paths of these materials is vital. Ensuring the connections between FRP composites and other materials can withstand these harsh environments is just as critical.

The application of existing standards and building codes, such as those issued by the U.S. Bureau of Reclamation [30] and American Concrete Institute [34] to the design and installation of FRP sheet piles is another important aspect to consider [4, 6-7, 35]. These standards and codes, which have been primarily developed based on the behavior of traditional materials like steel and concrete, may not fully account for the unique properties of FRP composites. Therefore, there is a need to develop and adapt these guidelines to better suit the use of FRP materials in construction, such as the Washington State Department of Transportation's design manual [4]. The study by Nagaraj and GangaRao [35] demonstrated the static behavior of pultruded GFRP beams, shedding light on the unique structural properties including shear influence and fatigue response of these materials that need to be taken into account in the design process.

The use of FRP composite sheet piles offers a promising alternative to traditional materials, providing advantages in terms of strength, durability, and resistance to environmental conditions. However, further research is needed to fully understand their performance under various conditions, to refine manufacturing processes, and to optimize their design for specific applications [14, 27, 29, 34, 36]. This study aims to contribute the state-of-the-art of FRP composite sheet piling by assessing the feasibility of laboratory testing of FRP sheet pile segments under cantilever loading, developing a test procedure that accurately determines the bending capacity simulating field conditions, and furnishing detailed instructions for replicating a test procedure valid for differing cross sections, sizes, and fiber volume fractions. A total of 16 FRP sheet pile tests were conducted, each featuring a cantilever beam bending induced under a static concentrated load pulled from the free end at the top of the pile, embedded a few feet below mud-line. The parameters measured during testing included load versus deflection and strain, with strains measured using strain gages bonded to sheet piles at several locations, in both the horizontal and vertical directions of the piles.

2 Experimental Program

Sheet pile walls represent a specific type of retaining wall comprised of interlocking, vertical pile segments that are driven into the ground to form a straight wall [6]. **Fig. 2** depicts two sheet pile cross sections with different interlocking mechanisms. These walls possess interlocking hinge mechanisms that enable continuous wall construction to a desired length, although they lack moment transfer capabilities. Depending on local soil conditions, the sheet piles can be driven deeper into the soil if the lateral support provided by the soil is insufficient to resist earth or water pressure. Despite their relatively low stiffness, which leads to larger deformations compared to other retaining wall types, sheet pile walls have gained popularity in waterfront environments due to their flexibility and ease of installation [31].

Cantilever walls are thin acting as vertical cantilever beams, with a rigid connection to the ground or attaching to a base that allows for a fixed connection. Cantilever walls are economically feasible to about 25’ in height. Cantilever walls without horizontal slabs or footers at the base of the wall rely entirely on the passive pressures exacted within the pile material. When the induced passive pressure is not sufficient to resist the active pressure, cantilever walls need to be anchored. In some cases, anchors are placed within concrete to minimize wall movement. Using the Earth Manual Standard [6, 37], one can immediately deduce the approximate permeability, shear strength, and volume change potential of a soil and how it may be affected by water, frost, and other physical conditions. Upon examination of soil properties, load distribution on the pile can be arrived at to characterize an economical sheet pile design.

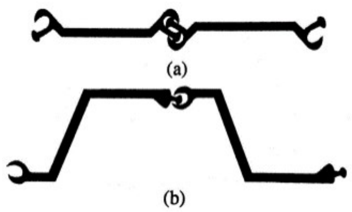

Fig. 2. Sheet pile connections.

Fig. 3. Sheet pile test in field (Photo Courtesy of Creative Composites Group).

In this study, FRP sheet pile segments under static flexural load testing in the field, are illustrated in **Fig. 3**. The experiments conducted consisted of four glass fiber reinforced polymer (GFRP) composite sheet pile modules (18 inches wide) acting as a thin-walled cantilever beam in vertical direction. Load was applied at the top of the sheet pile, as a retaining wall system, to simulate horizontal pressures in the field.

2.1 Specimen Details and Test Configuration

Four pultruded sections of Series 1580 SuperLoc™ Seawall Profile sheet piles segments of CCG (Creative Composites Group) were locked with one another, for each test, as shown in **Fig 4**. The sheet piles are manufactured using either vinyl ester or polyester matrix, reinforced with glass fibers and mats.

Several variations of the sheet pile testing (**Table 1**) in the Major Units Lab at West Virginia University, were carried out with variations in sheet pile geometric configuration, embedment material and height of load application.

Table 1. Sheet pile experiments (1 ft = 0.3048 m).

Base material	Number of Tests Conducted	Height of Load, ft	Load Application	Embedment Depth, ft
Sand	2	9.5	Actuator	5
Standard Concrete, No reinforcement	1	9.5	Actuator	2
Reinforced Concrete	1	9.5	Actuator	2
Concrete Mold with Elastomeric Padding	5	9.5-12.5	Actuator and Winch	2
Concrete Mold with Added Steel Channel	1	10.5	Winch	3.5
Steel Bin filled with Sand-Concrete Mixture	4	11.5-12.5	Winch	3
V-Test 1	1	12.5	Winch	3
V-Test 2	1	12.5	Winch	3

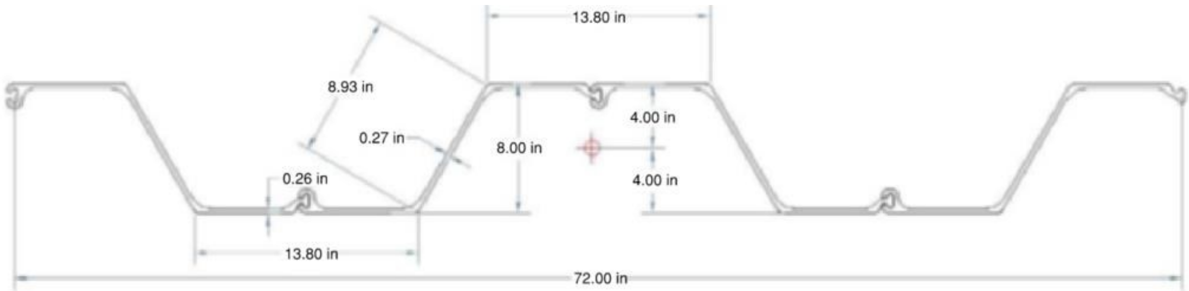

Fig. 4. Series 1580 SuperLoc™ polyester test specimen cross section (1 in = 25.4 mm).

Load was applied horizontally to each specimen so that cantilever loading was induced. A wale section was placed on either side of the test specimen to distribute load across the width of the sheet pile. Early methods featured an actuator mounted directly across the specimen (**Fig. 5**) and would pull the specimen at a specified rate of load per second. The actuator had a limited range of deflection, so a high-strength winch system was implemented. The winch was fixed to the ground with 3-inch structural bolts and the cable was placed inside of a pulley system suspended from an overhead crane so that load was applied horizontally (**Fig. 6**).

Fig. 5. Sheet pile test set up with Actuator.

Fig. 6. Sheet pile test set up with Winch.

Two wale sections were attached at the applied load location (see **Fig. 7**), on each side of the sheet pile with four ¾-inch bolts near the cantilever end. Stability is attained from the pressure resistance on both sides of the sheet pile beneath the dredge (mud)-line in the form of active/ passive pressures. The typical test specimen thickness is of the order of 0.265 inches (6.73 mm), in wall thickness. Four of these segments were joined by sliding the male end into the female end of the interlocking mechanism (groove and tongue). **Fig. 7** shows the wale sections mounted to top of the sheet pile, where loading was applied.

Fig. 7. Sheet pile test specimen.

2.2 FRP Composite Sheet Pile Section Properties

Table 2 shows section property values as provided by Creative Composites Group.

Table 2. Section property values as provided by Creative Composites Group.

Moment of Inertia	54.01 $\frac{in^4}{ft}$
Section Modulus	13.08 $\frac{in^3}{ft}$
Longitudinal Modulus	4250 ksi (29,303 MPa)
Transverse Modulus	1300 ksi (8963 MPa)
In-plane Shear Modulus	500 ksi (3447 MPa)
Longitudinal Poisson's Ratio	0.3

2.3 FRP Sheet Pile Material Properties

Procedure from ASTM D790-17 was followed on samples cut from the sheet pile to determine bending stresses to failure of the FRP sheet pile material at a coupon (4"x3/4"x1/4", i.e. 102mm x 19mm x6.35mm) level.

A bending modulus, E was calculated from load and deflection data, as given in **Fig. 8**, using classical bending deflection equation, which is $1.4x10^6$ psi (9653 MPa), while a typical stress vs strain of coupon from FRP sheet pile under bending is shown in **Fig.9.** Taking shear influence into account, a shear correction factor of 12% [35] can be applied to the longitudinal modulus of the compression flange. In this instance, the longitudinal modulus of the compression flange is the transverse modulus of the sheet pile specimen under bending which is perpendicular to the pull direction of a pultruded sheet pile section.

Three different approaches (coupon, 3 and 4 point bending of simply supported full sections) were used to find the transverse modulus of the test section. Approximate values for each of the moduli is 1.3, 1.6 and 1.8 msi. A value of 1.6 $m$si (11,032 MPa) was used as the transverse modulus for calculation purposes in this study.

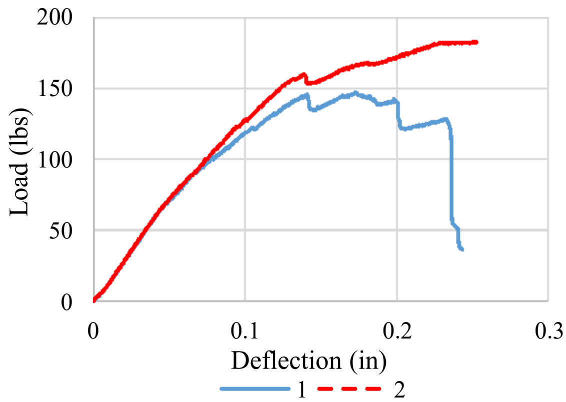

Fig. 8. Load vs Deflection from coupon #1 and #2 testing (1 lbs=0.454 kg; 1 in =25.4 mm).

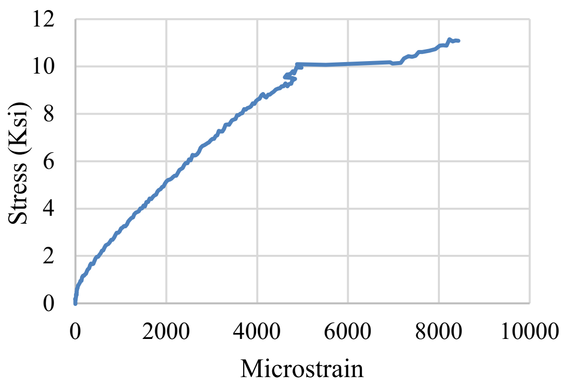

Fig. 9. Typical Stress vs Strain of coupon from FRP sheet pile under bending (1ksi=6.89 MPa).

2.4 Data Collection

Test data were collected from strain gauges, load cells, and a string pot for deflection using the Vishay data acquisition system 7000. Using Strain Smart Software, data was processed and exported to Microsoft Excel for further evaluation. The acquisition of deflection was recorded using a Celsco SP3-50 Compact String Pot for horizontal deflection measurements. For additional details of data collection, please refer to Wilt's thesis [11].

3 Experimental Results

Several sheet pile systems (4 or 5 modules were attached at the sides) were tested as cantilever beams under bending by embedding one end in: (a) Sand with wooden restraint at the bottom of the test floor, (b) fully encased in concrete, (c) encased in reinforced concrete, (d) concrete mold and surrounding sheet pile with elastomeric pad, and (e) sandy-concrete. The details of each type of test set up and data collection are described below.

3.1 Sand with Wooden Supports

Initially it was hypothesized that dry sand would suffice, surrounding the sheet pile and provide enough restraint for the pile. A wooden box (7’ length x 4’ width x 5’ depth) was constructed around the base of the test specimen so that approximately 12,000 pounds of sand could be poured to surround the pile. Five feet of the sheet pile was embedded in sand and approximately 5 feet of the sheet pile was free above the dredge or mud line. Wooden restraints were installed at the bottom of the bin to ensure that the sheet pile was restrained from horizontal movement.

The wooden members used to restrain the specimen at its bottom end caused local crushing of the pile. Upon removal of the wooden members, the pile was tested once more time in sand. When horizontal load was applied to the pile, a large bending moment was induced and caused the pile to rotate excessively, forcing the sand to heave due to the relatively small amount of sand, i.e., depth of 5 feet compared to 10+ feet in field conditions. **Fig. 10** shows a load-deflection curve for the test conducted in sand.

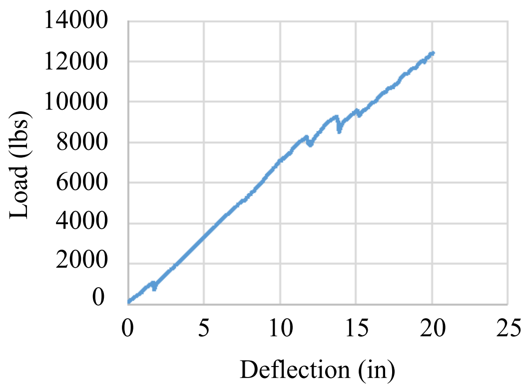

Fig. 10. Test in sand Load vs Deflection (1 lbs=0.454 kg; 1 in =25.4 mm).

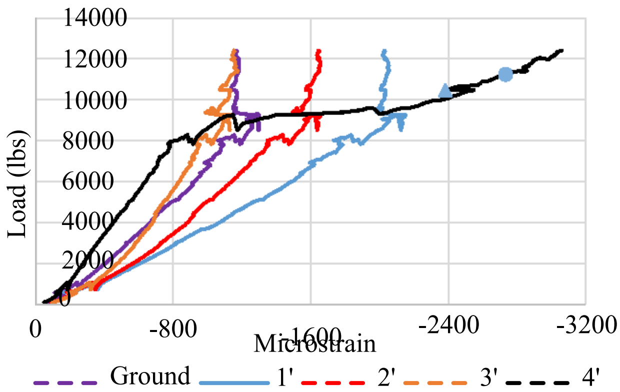

Fig. 11. Pile test in sand Load-Longitudinal Strain with gage mounted at 0 (ground), 1, 2, 3, 4ft beneath the dredge line (1lbs=0.454 kg; 1ft=0.3048 m).

The chart of loading vs. deflection is linear until the load dropped at 8,291, 9,277, and 9,408 pounds. Prior to the drop at 8,291 lbs of load, the slope of the response had increased. It is thought that the horizontal movement at this point had caused some of the load to transfer to the gantry crane that was supporting the actuator via a sling. The drop then occurred as the actuator had moved nearly 8 inches horizontally, causing a slip in the sling. The drop in the load-deflection curve that is shown at 9,277 lbs can also be observed in strain data as given in **Fig. 11**. The strain gages shown demonstrated a change at about 8,000 pounds of load, indicating that yielding had begun. The gage designation indicated the depth beneath the dredge line or at which the gage is located. A drastic change in strain was noticed at 4 feet beneath the dredge line.

Fig. 12. Concrete poured around specimen.

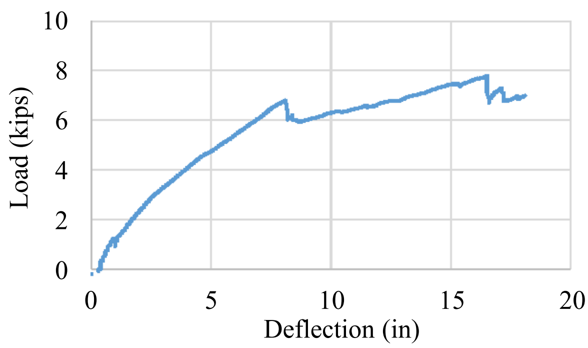

Fig. 13. Load vs Deflection concrete test (1 kips=454 kg; 1 in =25.4 mm).

3.2 Test with Plain Concrete Block

Following the experimental trial featuring sand, two-foot-deep plain concrete was chosen as a replacement. **Fig. 12** shows the 28 days strength of 2,850 psi concrete immediately after it was poured around the test specimen.

Fig. 13 shows load versus deflection curve that resulted from the initial concrete test. The pile began to deflect linearly until a small negative spike was noted, near 1 kip of load. The spike was attributed to the concrete at the base cracking, as was observed during the test. As loading continued, a more pronounced crack occurred near 6.8 kips of load, with final failure at 7.76 kips of applied horizontal load. This was indicated by a loud noise and visible cracking during the test and a rapid decrease in load applied followed by continued loading at a lesser rate. The concrete base was split into two parts because of the absence of any reinforcement in the concrete base, mostly restraining rotation of the sheet pile within the concrete block.

3.3 Reinforced Concrete

Steel reinforced concrete was constructed to prevent any cracking of the concrete base with the FRP sheet pile placed inside. **Fig. 14** shows the load versus deflection curve, with the maximum failure load at 8.7 kips.

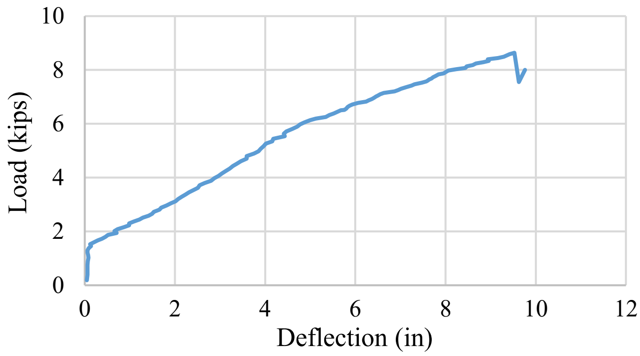

Fig. 14. Reinforced concrete Load vs Deflection (1 kips=454 kg; 1 in =25.4 mm).

A linear response in terms of deflection was observed as a result of transverse bending load applied to the test specimen, recognizing that an initial 1.5 kip load is needed to engage the load fixtures, i.e. total displacement to failure will increase, but not the load to failure. It is noted that reinforced concrete created a fully fixed base for the cantilever sheet pile unlike the field scenarios with compacted sands and clays as shown in Fig. 14 with load-displacement data. This level of fixity is not realistic in terms of field response of a sheet pile surrounded by soil. **Fig. 15** compares strain data 1 foot above the concrete block, with results from field testing, which implies that the concrete block restraining the sheet pile at the base is much more rigid than the *in-situ* soil conditions.

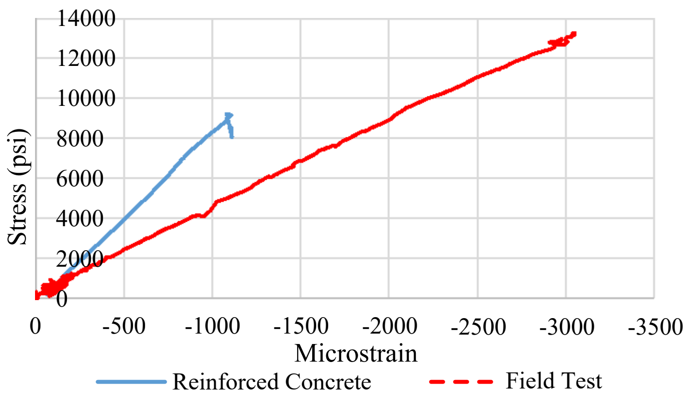

Fig. 15. Stress vs Strain comparison between reinforced concrete and field test (1ksi=6.895 MPa).

3.4 Concrete Mold with Elastomeric Pad

Elastomeric padding was used due to its ability to reduce fixity and allow the sheet pile to rotate about a pivot point below the dredge line. **Fig. 16** shows the mold that was used to restrain the test specimen at the bottom. Several tests were conducted by varying rubber padding within the mold to decrease test specimen fixity with the concrete base; but negligible load variations were noted, as shown in **Fig. 17**.

Fig. 16. Restraining structure with elastomeric padding.

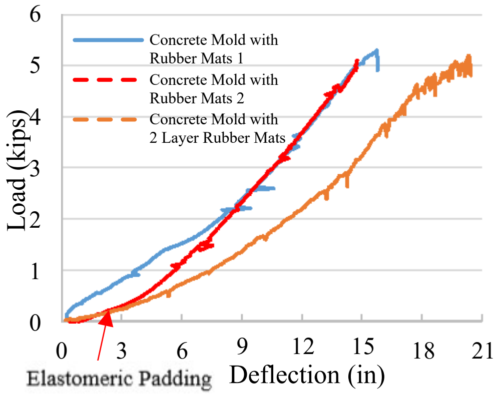

Fig. 17. Concrete mold Load vs Deflection (1 kips=454 kg; 1 in =25.4 mm).

3.5 Increased Embedment Depth with Sandy-Concrete

Additionally, embedment depth was increased to 40” by adding two 15-inch-tall steel channels on either side of the sheet pile and on top of the 25 inch concrete mold (**Fig. 18**). Concrete with added sand (called sandy-concrete) was used to fill the voids in between the channel and the sheet pile. This test procedure was conducted to increase the understanding of the depth needed to achieve sufficient loading and appropriate failure modes. **Fig. 19** shows the load versus deflection plot from two tests conducted with the channels added, i.e., increase in embedment depth.

Fig. 18. Increased embedment depth with two channels.

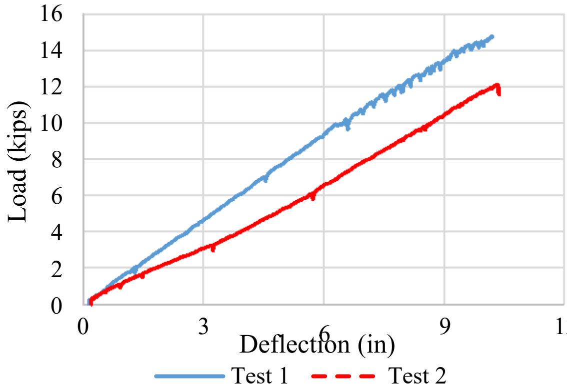

Fig. 19. Increased embedment depth Load vs Deflection (1 kips=454 kg; 1 in =25.4 mm).

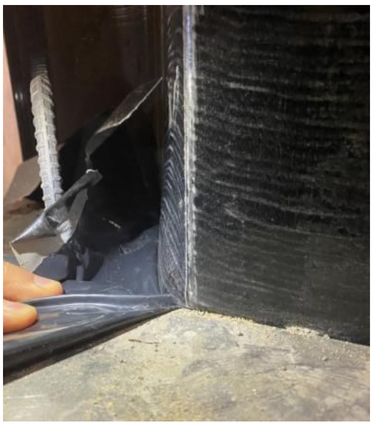

Fig. 20. Buckling about weak axis.

Fig. 21. Steel testing compression side (left) and sideview of testing bin (right).

Test 1 was conducted with a lever arm of about 7.5 feet (distance from load application to dredge line). With the increased embedment depth, the test specimen was able to withstand 14-15 kips of load prior to the test specimen reaching its ultimate value. The test was stopped because the winch, that was used to apply the load, was approaching its maximum capacity. To reduce the required load needed to fail the specimen, the lever arm was increased to 9.5 feet above the top of the concrete (dredge line) in Test 2, resulting in failure at 12 kips. Strain data were measured to understand the influence of embedment depth on the pile, which revealed that the test specimen was beginning to buckle about the weak axis as shown in **Fig. 20**.

3.6 Final Testing Fixture

Several factors went into the creation of the final test fixture. The fixture had to be large enough to contain a 6' wide, 8" deep sheet pile, rigid enough to resist around 15 kips of load while being extremely durable for repetitive use. Therefore, a customized steel angle-based bin (extending to a height of 3 feet) was manufactured by connecting to the test floor, as shown in **Fig. 21** (left). Three steel channels were bolted to the adjacent structural columns to form a wall on the tension side of the sheet pile. A ½" thick sheet of metal was welded to the channels to create a continuous and much stiffer (shear) wall as shown in **Fig. 21** (right). Once fully enclosed, a sheet pile section was placed in the center of this rectangle bin, and low-strength fill material encased the sheet pile. The fill material used consisted of 2 parts sand, 0.75 part 3000 psi concrete which is named as "sandy-concrete". This material provided adequate resistance to FRP sheet pile failure, simulating typical field conditions of silty or sandy clay.

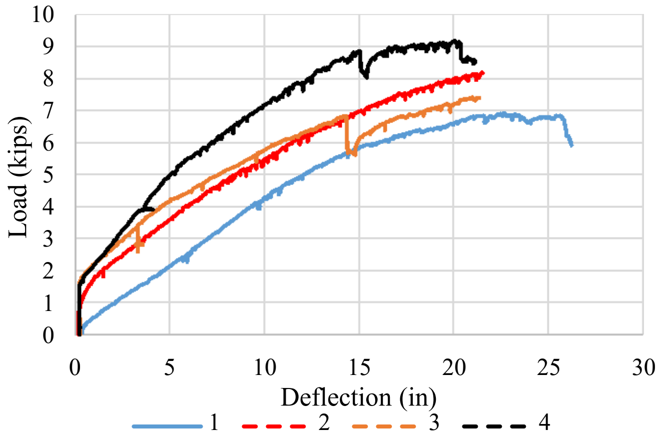

Fig. 22. Final test configuration Load vs Deflection for Tests #1 to 4 (1 kips=454 kg; 1 in =25.4 mm).

A total of four identical sheet piles (Series 1580 of CCG) were tested in the final configuration. Identical testing conditions took place for these tests. The only variability that took place was the differing lever arms from the first three tests and Test 4. The load-deflection results are displayed in **Fig. 22**. Three of the sheet pile test specimens had a total height of 13 feet (Test 1,2, and 3), with load applied at a height of 12 feet 6 inches from the bottom of the sheet pile and the 4th test specimen had load applied at 11 feet 6 inches.

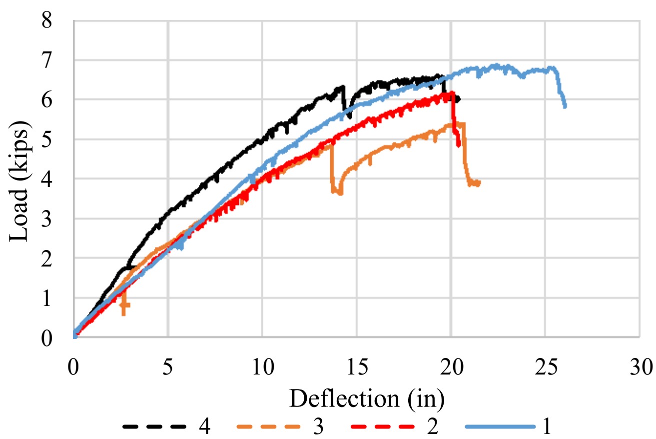

Fig. 23. Corrected Load vs Deflection for Tests #1 to 4 (1 kips=454 kg; 1 in =25.4 mm).

Tests 1, 2, and 3 (lever arm of 12 feet 6 inches) projected similar behavior in terms of load versus deflection. Test 4 differed slightly because of a decreased lever arm (11 feet 6 inches). Test 1 demonstrated an immediate response to loading due to a higher rate of loading applied from the start of the test. **Fig. 23** shows a version of the load vs deflection plot where all values have been adjusted so that (0,0) is the initial point when a response was measured. Tests 1, 2, and 3 are nearly identical due to the similar rate of loading. The response of Test 4 shows that a decreased lever arm resulted in increased stiffness, as expected.

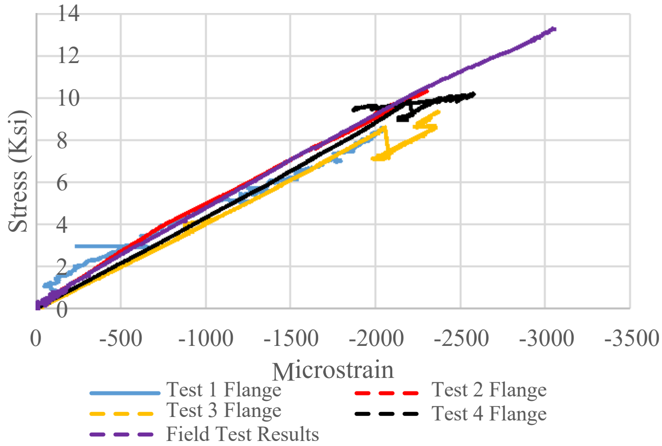

Fig. 24. Flange strain data compared with those from field test (1ksi=6.895 MPa).

The results from **Fig. 23** clearly show the degree of similarity in load-deflection response between each test. Strain data shown in **Fig. 24** and Fig. 25 provide additional evidence of the consistency that was observed with each of the final tests, including the responses that are similar to field test data.

Fig. 24 and **Fig. 25** show the longitudinal strains (compression zone) occurring on the interior flange - web junction for each of the four trials. **Fig. 24** includes field testing stress-strain data from the same location. The gages were all placed 1 foot above the dredge line surface. This location indicates the influence that the embedment material has on the test specimen. A slope in the stress-strain curve that is similar to the field testing results signifies that the sheet pile was responding as it would under field conditions without excess influence from embedment material. **Fig. 26** is an image of failure from Test 3 and representative failure of all four tests.

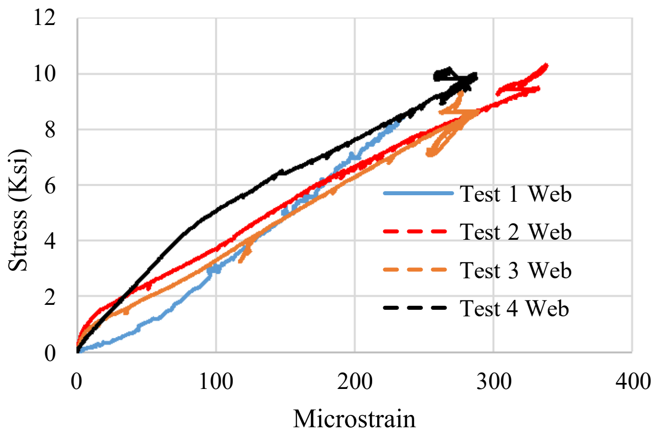

Fig. 25. Web strain data (1ksi=6.895 MPa).

Fig. 26. Sheet pile failure.

Each experiment showed clear signs of failure (fiber separation at web-flange junction parallel to the pile's longitudinal axis) about the weak axis of the pile as well as longitudinal separation at depths close to the dredge line. The low transverse modulus coupled with local stress concentration is the cause of this failure.

3.7 Variability in Sheet Pile Cross Section

To achieve the goals set for the test, alternate specimens were tested. The test denoted as V-Test 1 features 4 sections of the EverComp 26.1 (**Fig. 27**) joined together, with dimensions shown in **Table 3**. The test denoted as V-Test 2 is comprised of two EverComp 47.5 sections (**Fig. 28**). **Fig. 27** and **Fig. 28** are the cross-sectional profiles as provided by the manufacturer.

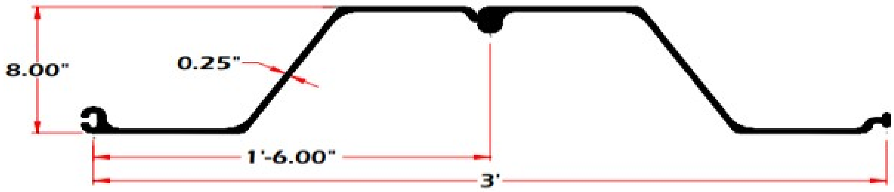

Fig. 27. EverComp 26.1 Sheet Pile Cross Section (1 in =25.4 mm).

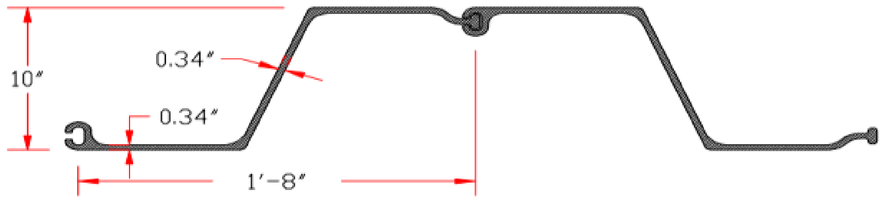

Fig. 28. EverComp 47.5 Sheet Pile Cross Section (1 in =25.4 mm).

Table 3. EverComp sheet pile properties (1 msi=6985 MPa).

Property	V-Test 1	V-Test 2
Longitudinal Modulus (psi)	4.2×10^6	3.6×10^6
Transverse Modulus (psi)	1.7×10^6	1.4×10^6
Longitudinal I $\left(\frac{in^4}{ft}\right)$	52	114
Distance from neutral axis to furthermost fiber c (in)	4	5

3.7.1 V-Test 1

The first test was nearly identical to the sheet pile from previous tests. The pile was pulled from a height of 13 feet after embedding in 3 feet of the sandy-concrete media as shown in **Fig. 29,** with the test results shown in **Fig. 30** and **Fig. 31**.

Fig. 29. Set up with V-Test 1

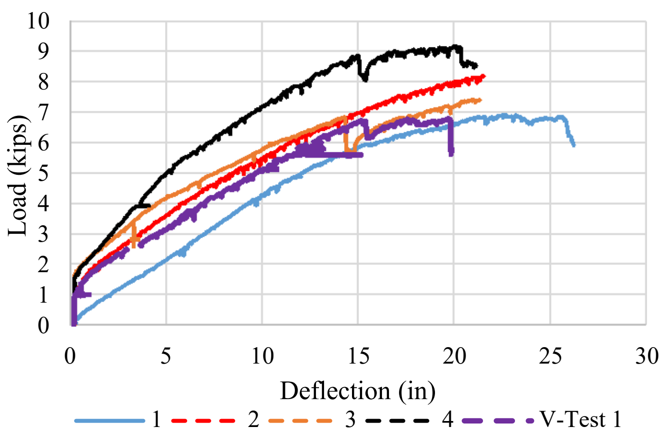

Fig. 30. Load vs Deflection data for Tests #1 to 4 and V-Test 1(1 kips=454 kg; 1 in =25.4 mm).

Testing revealed that similar properties led to similar load-displacement/ strain responses above the dredge line. **Fig. 32** shows the failure response of V-Test 1 specimen which is similar to Tests 1 thru 4. The pile has shown that the low transverse modulus cannot withstand the bending moment exerted on it from soil reaction and is consistently the initial mode of failure.

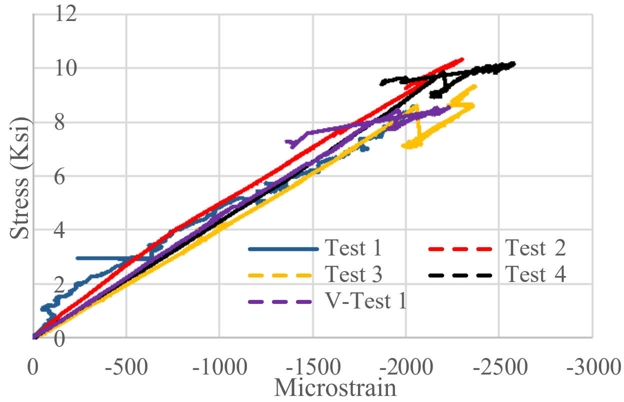

Fig. 31. Longitudinal flange strain data (1ksi=6.895 MPa).

Fig. 32. V-Test 1 sample failure.

3.7.2 V-Test 2

The second set of the two types of sheet piles from a different manufacturer was tested in the same fashion as all of the other specimens. This sheet pile, however, featured only two segments. The segments (**Fig. 28**) had considerable variability in material properties. **Fig. 33** shows the load vs displacement response of V-Test 2.

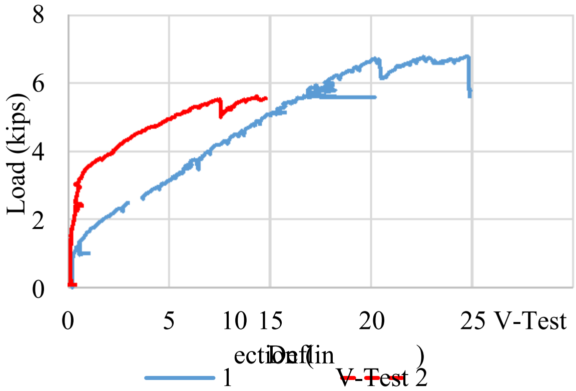

Fig. 33. V-Test Load vs Deflection data (1 kips=454 kg; 1 in =25.4 mm).

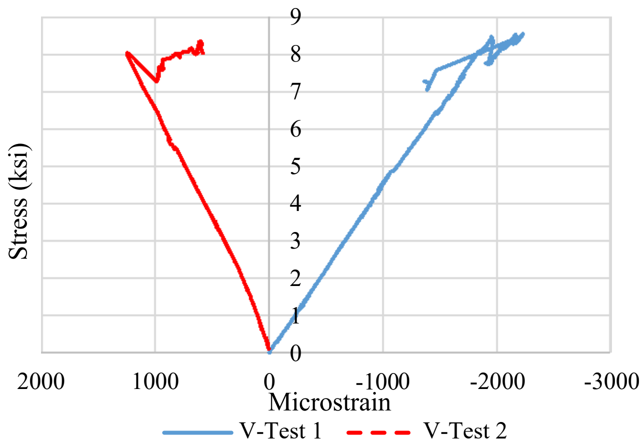

Fig. 34. Longitudinal strain 1-foot above dredge line (1ksi=6.895 MPa).

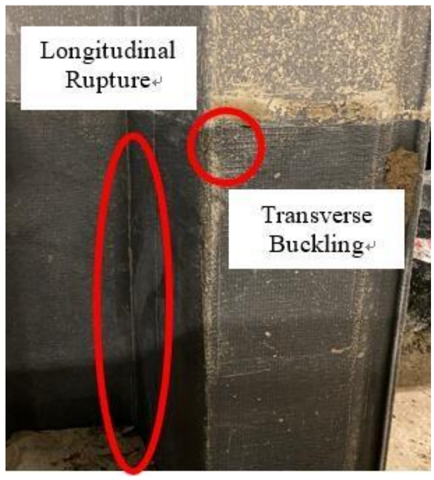

Fig. 35. V-Test 2 sample horizontal and vertical failure.

Fig. 33 compares the load versus displacement results from the two V-Tests and the increase in flexural rigidity from V-Test 1 to V-Test 2 is apparent. **Fig. 34** compares the flange strains on the compression side (horizontal direction) at 1 foot above the dredge line from V-Test 1 and V-Test 2. The differed location (compression side versus tension side) with respect to the neutral axis led to opposing signage, but the values recorded are still useful. Less strain was exhibited on V-Test 2 and the pile showed a slightly higher slope on the stress-strain curve. **Fig. 35** shows an image of failures that had occurred on V-Test 2's specimen.

4 Discussions and Theoretical Analysis

The purpose of this research is to develop a standardized test procedure to determine the resisting moment capacity of FRP composite sheet piles. Specifically, the moment induced at any given point on a sheet pile is proportional to the stress experienced in conjunction (interaction) with soil pressures and the failure stress is a function of the failure mode. The cantilevered FRP sheet pile fixed at the bottom with a sand-concrete mixture of ~70 psi (0.48 MPa) compressive strength (shear strength of ~35 psi) that is buried by about 3 feet (0.91 m) was tested under static loads, while the free-standing section of the sheet pile extended an additional 10-12 feet (3-3.66 m) above mud line. Strain gages and LVDTs were installed strategically on pile surface (above and below mud line) to collect strain and deflection data during testing to establish load vs deformation response up to and beyond the peak induced stress.

Failure occurs along the weak bending axis of the sheet pile when flexural stress is incurred on the test specimen. A net pressure distribution diagram along the length of the pile is created using strain data to compare with the literature data. The load-strain diagrams indicate pressure along the depth of the sheet pile that is buried about 3' below mud line. Several sheet piles have been tested with consistent results that correlated well with the proposed theoretical sheet pile design procedures developed as a part of this research. Results from this study suggest that the test procedure refined herein can become a useful resource to assist engineers in designing efficient sheet pile structures. The proposed test procedure will be a basis to develop ASTM standard to establish load capacity of sheet piles as a function of its geometric properties, soil properties and embedment length.

Additional observations from this experimental study are: 1) An embedment material with sufficient shear strength must be established, 2) The load applied to the sheet pile generated large reactionary forces at the base of the pile; if the media surrounding the test specimen does not have adequate shear strength, the sheet pile will never reach optimal load, and 3) The material used in the final test procedure was 0.75 parts concrete (3,000 psi, i.e. 20.68 MPa) versus 2 parts sand. Through multiple forms of test and analysis, it was determined that the cohesion of this material was 35 psi [11].

Different degrees of fixity occurred as a result of different embedment material properties. Sheet piles derive their stability when horizontal force is applied, and they have certain freedom to deflect as discussed earlier. If the test specimen was embedded in concrete of high compressive strength (4000 psi, i.e. 27.58 MPa), no signs of cracking were noted after applying 8.6 kips (3904 kg) of load. The reinforced concrete block provided considerably more fixity for the sheet pile than any other embedment material; however unrealistic under field conditions. Another example of this was the lower strain to failure, i.e., less strain equates to less deformation. This is characteristic of a rigid cantilever support as opposed to a sheet pile embedded in flexible soil. This observation proved the validity of embedment material chosen for the final test configuration.

Stress concentrations occur at the corners of the web and flange sections, leading to corner failures. While the dominant mode of failure may have occurred about the transverse axis for most specimens, nearly all tests showed signs of separation or cracking in the corners. Upon the observance of the phenomenon of cracking at corners near the dredge line, strain gages were placed on a test specimen near the dredge or mud line to confirm the assumption that stress concentrations are present [11].

This study has successfully established and validated a consistent test configuration and methodology for determining the loading capacity of FRP sheet piles. Additionally, a procedure for the theoretical analysis of FRP sheet piles has been developed. The theoretical procedure's consistency was evaluated using data from Wilt et al. [11]. A brief discussion on theoretical analysis is presented below. However, a comprehensive description of the theoretical work will be provided in follow-up technical papers. These papers will demonstrate the accuracy and usability of the design and analysis equations developed throughout this study.

An in-depth analysis on strain data at several locations on the sheet pile provided key insight to the failure behavior of the sheet pile. Strain results near the corners of the sheet pile cross section revealed that strain readings were approximately 3-4 times higher than strain readings at the same height on the center of the web or flange section. Formulas were developed to utilize strains taken from strategic locations to create design equation for both the longitudinal and transverse axes [11]. Additionally, a procedure was developed to analyze the shear capacity of the material used to retain the sheet pile in the final test configuration.

Shear capacity of the embedment material surrounding a specimen can be calculated with Eq. (1):

$$\tau_{\mathrm{f}} = \frac{\sigma_1}{2} = \frac{q_{\mathrm{u}}}{2} = c_{\mathrm{u}} \tag{1}$$

where, τ_{f} = Shear Strength (psi) , σ_1 =Principal Stress (psi), q_{u} =Normal Stress (psi), c_{u} =Cohesion (psi).

Once satisfied, the pressure acting on a given location can be calculated with Eq. (2) as derived in the reference [11]:

$$w_{\mathrm{f,w}} = \frac{10EI\varepsilon_{\mathrm{f,w}}}{l_{\mathrm{f,w}}{}^2 c} \tag{2}$$

where, w_{f} = Uniform pressure on flange (lb/in/in), w_{w} = Uniform pressure on web (lb/in/in), l_{f} = Length of flange (in), l_{w} = Length of web (in), c= Distance from neutral axis to furthermost fiber (in),

E = Bending Modulus (psi), I = Unit Area Moment of Inertia $(\mathrm{in}^4/\mathrm{in})$, ε_{f} =Flange strain at peak load (με), ε_{w} =Web strain at peak load (με).

Once the pressure is obtained from Eq. (2) the resultant force can be derived to obtain the maximum load capacity of the test specimen about the transverse axis.

The maximum load capacity of the longitudinal axis can be calculated with Eq. (3):

$$\varepsilon_{\mathrm{f}} = \frac{\sigma}{E} = \frac{M_{\max} c}{E_L I} \tag{3}$$

where, σ = Bending Stress (ksi), E_L = Longitudinal Modulus (ksi), $M_{\max}$ = Maximum bending moment (ft-kips), l= Length of specimen (in).

Additional equations have been developed and can be found in the reference [11]. These equations offer the capability to compare theoretical values with the test results obtained with strain gauges. Moreover, these procedures can be utilized, as demonstrated in example problems, to establish an adequate test procedure with the appropriate embedment material, depth, and cross sectional property variations of test specimens.

5 Conclusions

This paper presents an experimental study on evaluation of FRP composite sheet piles under cantilever loading. This study has successfully established and validated a consistent test configuration and methodology for determining the loading capacity of FRP sheet piles. Additionally, a procedure for the theoretical analysis of FRP sheet piles has been developed and a comprehensive description of the theoretical work will be provided in follow-up technical papers. The test methodology with emphasis on different failure modes includes the selection of an appropriate embedment material with sufficient shear strength to withstand the large reactionary forces generated at the pile base, understanding the different degrees of fixity resulting from embedment materials with varying properties, and recognizing the stress concentrations that occur at the corners of the web and flange sections.

It was found that the stability of sheet piles largely depends on the pressures generated within the soil when horizontal force is applied, necessitating certain flexibility to deflect. Embedment in high compressive strength concrete significantly increased the pile's fixity, resulting in lower strain to failure - a characteristic of a fixed cantilever rather than a soil-embedded sheet pile. Observations during testing confirmed stress concentrations at corners near the mud line, a critical factor in sheet pile design and analysis.

Sheet pile structures, whether temporary or permanent, play a vital role in various infrastructural projects, including below-grade parking structures and sea walls. The ability to design these structures efficiently and effectively is crucial for their successful implementation and operation. Therefore, the developed standardized test procedure for determining the resisting moment capacity of FRP composite sheet piles represents a significant step forward in the field. This procedure will not only facilitate the design of efficient sheet pile structures but also serves as the basis for developing ASTM standards for determining the load capacity of sheet piles as a function of their geometric properties, soil properties, and embedment length.

Funding Statement

This work is sponsored by Creative Composites Group through the NSF Industry- University Collaborative Research Center Membership Program at West Virginia University. The NSF IUCRC Center for Integration of Composites into Infrastructure (CICI) is supported by NSF through Award #1916677.

Credit authorship contribution statement

Joshua Wilt: Investigation, Data analysis, Development of technical report. **Ruifeng Liang:** Project management, Investigation, Manuscript development**. Hota GangaRao**: Project development and direction, Test method design, Investigation, Data analysis, Manuscript development. **Jeremy Mostoller:** Supply of test specimens, Project development, Discussion on test method development and test results.

Conflicts of Interest

The authors declare that they have no conflicts of interest to report regarding the present study.

References

[1] GangaRao HVS, Prachasaree W. FRP composite structures: Theory, fundamentals, and design. CRC Press, 2021. https://doi.org/10.1201/9781003196754.

[2] Rajak DK, Pagar DD, Menezes PL, Linul E. Fiber-reinforced polymer composites: Manufacturing, properties, and applications. Polymers 2019; 11 (10):1667. https://doi.org/10.3390/polym11101667.

[3] Wang J, Liu W, Liang R, GangaRao HVS, Wan L. Analytical and experimental study on flexural behavior of pultruded fibre reinforced polymer sheet piles. Journal of Composite Materials 2016; 50 (24): 3415-3429. https://doi.org/10.1177/00219983156213.

[4] Washington State Department of Transportation Design manual (M 22-01.19). Olympia, WA, 2020. https: //wsdot.wa.gov/publications/manuals/fulltext/M22-01/730.pdf

[5] Das BM, Sivakugan N. Principles of foundation engineering. Cengage learning, 2018.

[6] USACE. EM 1110-2-2504: Design of sheet pile walls. US Army Corps of Engineers, 1994.

[7] Technical Supplement 14R Design and Use of Sheet Pile Walls in Stream Restoration and Stabilization Projects, Stream Restoration Design, National Engineering HandbookVolume 654, 31.

[8] Guades E, Aravinthan T, Islam M, and Manalo A. A review on the driving performance of FRP composite piles. Composite Structures 2012; 94 (6): 1932-1942. https://doi.org/10.1016/j.compstruct.2012.02.004.

[9] Lampo R, Noske T, Bamo D, Busel J, and Maher A. Development and Demonstration of FRP Composite Fender Loadbearing, and Sheet Piling Systems. Construction Engineering Research Lab (Army) Champaign Il, 1998.

[10] Fang H, Bai Y, Liu W, Qi Y, and Wan J. Connections and structural applications of fibre reinforced polymer composites for civil infrastructure in aggressive environments. Composites Part B: Engineering 2019; 164: 129-143. https://doi.org/10.1016/j.compositesb.2018.11.047.

[11] Wilt JL. Design of bending moment and load capacity test for FRP sheet piles. Graduate Theses, Dissertations, and Problem Reports #10201.West Virginia University, 2021. https://researchrepository. wvu.edu/etd/10201/

[12] Giroux C. and Shao Y. Flexural and shear rigidity of composite sheet piles. Journal of Composites for Construction 2003; 7 (4): 348-355. https://doi.org/10.1061/(asce)1090-0268(2003)7:4(348).

[13] Shao Y, and Shanmugam J. Moment capacities and deflection limits of PFRP sheet piles. Journal of Composites for construction 2006; 10(6): 520-528. https://doi.org/10.1061/(asce)1090-0268(2006)10:6 (520).

[14] Chen Y. Local buckling behaviour of pultruded FRP composite sheet piles subjected to uniform pressure,

2005.
[15] Noh J, Ghadimi B, Russo S, and Rosano M. Assessment of FRP pultruded elements under static and dynamic loads. Composite Structures 2018; 202: 17-28. https://doi.org/10.1016/j.compstruct.2017.09.107.
[16] Boscato G, Mottram JT, and Russo S. Dynamic response of a sheet pile of fiber-reinforced polymer for waterfront barriers. Journal of composites for construction 2011; 15 (6): 974-984. https://doi.org/10.1061//(asce)cc.1943-5614.0000231.
[17] Wang J, GangaRao H, Liang R and Liu W. Durability and prediction models of fiber-reinforced polymer composites under various environmental conditions: A critical review Journal of reinforced plastics and composites. Journal of Reinforced Plastics and Composites 2016; 35 (3): 179-211. https://doi.org/10.1177/0731684415610920
[18] Wang J, GangaRao H, Liang R, Liu W, Zhou D, Fang Y. Durability of glass fiber-reinforced polymer composites under the combined effects of moisture and sustained loads. Journal of reinforced plastics and composites 2015; 34 (21): 1739-1754. https://doi.org/10.1177/0731684415596846
[19] Kouadio KSP. Durability of fiberglass composite sheet piles in water, 2001.
[20] Murthy, VNS. Geotechnical engineering: principles and practices of soil mechanics and foundation engineering. CRC press, 2002.
[21] Das BM, Principles of geotechnical engineering. Cengage learning, 2017.
[22] Wang Z, Wu S, Weng K, Yao W, Xu S, Ding Z. Vertical and lateral bearing capacity of FRP composite sheet piles in soft soil. Advances in Civil Engineering 2020; 2020: 1-10. https://doi.org/10.1155/2020/8957893
[23] King GJW. Analysis of cantilever sheet-pile walls in cohesionless soil. Journal of geotechnical engineering 1995; 121 (9): 629-635. https://doi.org/10.1061/(asce)0733-9410(1995)121:9(629).
[24] Choudhury D, Singh S, Goel S. New approach for analysis of cantilever sheet pile with line load. Canadian Geotechnical Journal 2011; 43: 540-549. https://doi.org/10.1139/t06-018.
[25] El-Hanafy AM, AbdelAziz MH. Effect of using cemented sand as a replacement layer beneath a strip footing. HBRC Journal 2021; 17 (1): 1-17. https://doi.org/10.1080/16874048.2020.1863050.
[26] GuhaRay A, and Baidya D K. Reliability-based analysis of cantilever sheet pile walls backfilled with different soil types using the finite-element approach. International journal of Geomechanics 2015; 15 (6): 06015001. https://doi.org/10.1061/(asce)gm.1943-5622.0000475.
[27] Gopal Madabhushi SP, and Chandrasekaran VS. Rotation of cantilever sheet pile walls. Journal of geotechnical and geoenvironmental engineering 2005; 131(2): 202-212. https://doi.org/10.1061/(asce)1090 - 0241(2005)131:2(202).
[28] Terzaghi K. Large retaining wall tests. I. Pressure of dry sand. Eng. News-Rec 1934; 136-140.
[29] Fabien D. Finite Element Analysis of Composite Sheet Piles Subjected to Uniform Load and Harsh Environments (Doctoral dissertation, McGill University Montreal, Canada), 2005.
[30] U.S. Bureau of Reclamation. E-7 Seismic Evaluation of Retaining Walls, US Department of The Interior, 2019.
[31] Bilgin Ö. Numerical studies of anchored sheet pile wall behavior constructed in cut and fill conditions. Computers and Geotechnics 2010; 37 (3): 399-407. https://doi.org/10.1016/j.compgeo.2010.01.002
[32] Liang R, Gangarao H. Development and evaluation of load-bearing fiber reinforced polymer composite panel systems with tongue and groove joints. Sustainable Structures, 2021, 1 (2): 000008. https://doi.org /10.54113/j.sust.2021.000008
[33] Liang R, Gangarao H, Clarkson JD. Worldwide overview of composite applications for waterway infrastructure. Journal of Advanced Materials 2020; 121-133.
[34] ACI Committee 318. Building code requirements for structural concrete: (ACI 318-95); and commentary (ACI 318R-95). Farmington Hills, MI: American Concrete Institute, 1995.
[35] Nagaraj V and GangaRao HVS. Static behavior of pultruded GFRP beams. Journal of Composites for Construction 1997; 1 (3): 120-129. https://doi.org/10.1061/(asce)1090-0268(1997)1:3(120).
[36] Timoshenko S, Woinowsky-Krieger S. Theory of plates and shells, 1959.
[37] U.S. Bureau of Reclamation. Earth Manual, US Department of the Interior, 1998.